Adaptive Positioning Systems Based on Multiple Wireless Interfaces for Industrial IoT in Harsh Manufacturing Environments

Abstract—As the industrial sector is becoming ever more flexible in order to improve productivity, legacy interfaces for industrial applications must evolve to enhance efficiency and must adapt to achieve higher elasticity and reliability in harsh manufacturing environments. The localization of machines, sensors and workers inside the industrial premises is one of such interfaces used by many applications. Current localization-based systems are unable to deal with highly variable conditions, meaning that the solutions working well in stationary systems suffer from considerable difficulties in harsh environments, such as factories. As a result, the precision of localization techniques is not satisfactory in most industrial applications. This paper fills in the existing gap between static approaches and dynamic indoor positioning systems, by presenting a solution adapting the system to highly changeable conditions. The proposed solution makes use of a Machine Learning-based feedback loop that learns the variability of the environment. This feedback makes continuous fingerprint calibration feasible even in the presence of different machines and Industrial Internet of Things sensors that introduce variations to the electromagnetic environment. This paper also presents a comprehensive indoor positioning system solution that reduces complexity of hardware, meaning that a multi-standard-transceiver infrastructure may be adopted with reduced capital and operational expenditures. We have developed the system from scratch and have conducted an extensive range of testbed experiments showing that the multi-technology transceiver feature is capable of increasing positioning accuracy, as well as of introducing permanent fingerprints calibration at harsh industrial premises.

Index Terms—Positioning system, Mahalanobis distance, calibration, industrial IoT, industrial interface.

I. INTRODUCTION

IN THE future, industrial robots will need to be flexible in order to be able to work on different products. Industrial processes can no longer be a series of defined-from-the-design static processes in which robots perform the same actions during their entire lifecycle. Flexibility in manufacturing is one of the main features of the Industry 4.0 concept and allows to enhance overall productivity, avoid stagnation and multiply the potential number of end-to-end processes. The main technological requirement for achieving the necessary flexibility of robots is that robots must not be restricted by any limitations or hindrances. Therefore, factories must be free from cables and wireless communications are a must in Industry 4.0. The 5G network is capable of implementing all-wireless fundamentals at new factories. 5G allows to give up wired connectivity in industries due to the fact that it is suitable for the implementation of Ultra-Reliable Low Latency Communications scenarios. These scenarios are crucial for the Industrial Internet of Things (IIoT) [1]–[3].

However, the challenges that wireless robots face at industrial premises are countless due to the harsh environment in which they operate. The management of industrial processes requires fast and precise responses of all elements connected to the system. Therefore, precise localization of all such elements of the wireless production environment is crucial in all industrial applications. Location-based services are crucial for both performance and safety. Precise robot localization is crucial for orchestrating all tasks that robots are required to perform in real-time, as machinery movements depend on the distance from various sensors. Precise robot and person localization is crucial for safety, when both people and machine share the same physical space [4]. Context-awareness is also crucial for maintenance-related activities performed at automated industrial premises, helping the maintenance personnel to navigate through the shop floor [5]

Production machinery and equipment poses numerous challenges when it comes to precise wireless communications, and, specifically, to localization technologies: electromagnetic compatibility, which cannot be taken for granted, multiple radio systems working within similar radio frequency bands, echoes and absorption of electromagnetic signals, etc.

Traditional indoor localization (positioning) systems, such as those based on Time of Arrival or Received Signal Strength in Bluetooth or WiFi, are too imprecise in industrial environments [6], [7]. Newer positioning techniques using different radio technologies have appeared in industrial applications. These work with short range radio technologies on separate radio spectrum bands. The most popular are Ultra-wideband (UWB) [8] and Radio-Frequency Identification (RFID) [9].

UWB uses Time of Flight, which is an adaptation of the classic Time of Arrival systems. Time of Flight estimates the light transit time between two points, and Time of Arrival estimates the transit time of other electromagnetic signals between two points. UWB is very precise (accuracy of approx. 30 cm), but highly cost-ineffective. Moreover, it requires a line-of-sight between the transceiver and the receiver, which is very difficult in flexible manufacturing (Industry 4.0). RFID-based positioning is cost-effective, but the range is very short (around 1 m); as most industrial applications require much longer ranges, its use is rather marginal in factories. Because of the difficulties experienced in implementing these new technologies, the investigation is coming back to classic positioning systems and to improving their features for industrial applications [10]–[12].

In this paper, we present a system used for positioning industrial elements, based on the Received Signal Strength (RSS) technology deployed in harsh and changing environments. The novelty of this solution compared to other research studies is that the proposed system is capable of adapting to changing conditions prevailing in industrial environments. This means that it is capable of overcoming the limitations that prevent it from being used in Industry 4.0. The antennas continuously receive signals from sensors and use Machine Learning to continuously estimate the position of anchor elements in the area. Machine Learning plays a crucial role in changing the conditions, since it is capable of adapting the results to specific environments. Our algorithm integrates new and old data, such that it allows to adjust the setup to the current state of the space under analysis (considering new objects appearing in the industrial setting and causing interference, generating echoes, signal shadows, etc.). A big factory with free-moving (wireless-guided) robots is a typical scenario in which our mechanism may outperform other positioning systems.

The main contributions of this paper are (1) the introduction of a Machine Learning algorithm to adapt the fingerprints of Received Signal Strength (RSS) measurements of the signal sent by the manufacturing machines or sensors and received by multiple transceivers located within the analyzed space; (2) the introduction of low-cost transceivers for positioning purposes across industries. Specifically, we propose a new approach to transceiver development that consists in separating radio signal processing from message processing. The former functionality is almost technology-independent (considering technologies operating in the 2.4 GHz band), whereas the latter depends on the technology used; and (3) the limitation of radio interferences thanks to the integration of multi-technology with several radio interfaces. Our system operates with different technologies (Wi-Fi, Bluetooth, RFID and other

beacon-based solutions) and is open to the adoption of other technologies which could be introduced simply by establishing communication with the use of appropriate frequencies. The sensor positioning process is integrated with the technology-dependent modules, allowing for the implementation of various technology-dependent fingerprint maps.

As a result, we present a solution based on medium-range technologies, achieving the level of accuracy comparable to that of UWB (at the range of 0.4 m), while maintaining limited costs (Capital Expenditures) and ensuring effective power consumption (low Operational Expenditures). Finally, our solution requires no action on the part of the tracked sensors, allowing simultaneous positioning with the use of several radio technologies operating in the 2.4 GHz band, with measurements performed in an environment with a dense network of transceivers, therefore limiting the impact of radio interference between specific technologies and devices.

The next section presents other indoor positioning solutions, with the majority of them based on Wi-Fi radio technology. Section III presents our solution to such systems, based on multi-technology multi-antenna hardware and relying on an advanced fingerprints algorithm with system adaptation feedback, combining calibration and positioning phases. In Section IV, we present a long list of trials conducted with the use of our solution that, on the one hand, show the operational range of the system, and, on the other, demonstrate its accuracy. In Section V, future work is discussed.

II. STATE OF THE ART

The specificities of industrial environments pose several challenges to location-based systems. New technologies, such as UWB, have been introduced, but their high costs and difficulties in adapting them to very changing environments (e.g. industrial settings) considerably restrict their development.

The majority of solutions positioning indoor devices with the use of technology-based monitoring rely on the 802.11 network (Wi-Fi). The advantage of that approach consists in a relatively low-cost of its implementation compared to other wireless technologies, because many Wi-Fi network locations already exist within a specific the infrastructure. Although the Wi-Fi standard did not provide for functional positioning, its radio signals may be used to assess the location based on Received Signal Strength (RSS), enabling to identify the distance between the devices and their base stations and, in consequence, the location of such devices (please note that the word "device" used in this paper refers to industrial machines, factory workers' mobile phones, sensors used in IIoT or any other hardware that must be localized) in an indoor environment. A similar technique may be used in other technologies.

RSS-based positioning often requires a compensation model for minimizing RSS measurement errors and space variations [13]. The authors of [14], [15] propose to position the devices by integrating shadowing models into their estimations. In the same way, the solutions of [16], [17] compute the position by means of a propagation model of the signal. The development of an accurate propagation model for each Wi-Fi access point (AP) within a real environment is

extremely difficult. Therefore, the majority of solutions are burdened with relatively high accuracy positioning errors [18]. An interesting approach based on graphical signal propagation modeling (3D graphic model) has been presented in [19]. The idea is to model propagation by analyzing the environment. This approach requires considerable computational power, but offers a short deployment time (it may be used practically from the very the beginning). This system achieves acceptable results in simple scenarios, however it is not clear whether its deployment is feasible in real life scenarios.

Fingerprinting is another common localization method that is based on measuring RSS [20]–[25]. The authors of [20] use machine learning methods to localize minimum variable environments, whereas in [21], the authors propose deep learning. Paper [22] proposes that localization be based on employing fuzzy logic, while the method proposed in [23] is based on deep neural networks. In [24], ï'ngerprints are estimated using latent semantic analysis (LSA) and singular value decomposition (SVD). All these solutions envisage only one type of wireless technology (Wi-Fi, BLE, etc.). This type of localization is based largely on the use of empirical data. Under this method, localization is usually carried out in two phases: calibration and positioning. In the calibration phase, the APs measure RSS of the signal emitted by a test device. The average from several measurements is used as an RSS reference value. Each test becomes a point on the radio map in which individual locations are defined by geographical coordinates and by the specific value of feed for each AP. During the positioning phase, the mobile device measures the value of RSS at an unknown location and uses an algorithm to estimate the location, using the radio maps that have been created previously. Because factory premises are characterized by unique features affecting propagation of the signal, one may assume that each location may be determined by a unique combination of RSS. Such an assumption is faced with numerous obstacles during real-life implementation, since the calibration conditions and positioning vary significantly, as will be shown below. All that considered, one needs to mention an interesting approach presented by Pendão and Moreira in [26]. They proposed to calibrate the system under the same conditions as prevail during localization phase, by using some anchor nodes that are sniffed (as in our solution) and their position is estimated. This estimated position is used to estimate the position of the device (e.g. machine, sensor). The results shown in [26] reveal that the solution achieves the objectives (calibration and positioning are performed under similar conditions), but fails in achieving a decisively higher level of accuracy due to the fact that the estimation of the device position is based not on real position of anchor nodes, but on their estimated position. In this sense, our approach is a step forward and achieves better results, however we need a more complex infrastructure by adding, to the infrastructure, these anchor nodes (in [26] the role of anchor nodes was played by devices).

Considering the accuracy of the fingerprinting measurement method, correlation between the result of RSS measurements and the individual items on the radio map seems to be the key element. In practice, it all boils down to determining the distance between the two abovementioned points which, in statistical terms, maps contributions of the individual components and uses the correlation between them. In this context, it is essential to select the appropriate measure of distance, as pointed out by the authors in [27], because positioning accuracy is closely related thereto. The authors of [28] analyze two different distance measurements in terms of their application to fingerprinting-based positioning using Wi-Fi networks and magnetic fields. These are Euclidean distance and Mahalanobis distance, showing that the highest accuracy was achieved, in both cases, by using Mahalanobis distance. Similar results are obtained in [29]. In [30], the authors analyze fingerprinting localization with RSRP signals (RSS standardized for LTE) by means of MD and Kullback-Leibler divergence methods, setting MD as a par excellence solution, showing that only specific situations may be overcome. In [31], MD is used to filter those values that are severely different from standard values, based on that probability of this distance being different from others. The use of Mahalanobis distances (MD) in several other solutions that do not rely on fingerprints [30]–[33] is a confirmation of this thesis. In [32], MD and Euclidean distance are compared for localization classification scope. In [33], effectiveness of MD is compared with vs Euclidean distance by means of RFID-based location, showing, in both cases, the superiority of MD.

A number of enhancements designed to increase accuracy have been proposed [34] over the recent years. These extensions generally concern volatility of RRS values, often encountered in real conditions. Therefore, other sources of measurements are added in order to increase their accuracy. These include, for instance, data received from the Inertial Measurement Unit (IMU) module [35], which is an accelerometer or a magnetometer, or from ultrasound [36] devices. However, it is worth mentioning that in these approaches ([35] and [36]), the measurement data is obtained with the use of the device (which actively participates in performing the measurements, see [17]) whose consent might exclude the possibility of using this method for information-related purposes of vendor. In fact, active measurements provide higher accuracy levels but require the implementation of a positioning protocol between the sensor and the antenna in order to exchange information about the location. Instead, in passive measurements, localization is based solely on measurements taken at the transceiver side while establishing the connection between the device and the base station, i.e. before any application is run on the machine. Many other localization methods relying on active device participation exists. The most important of these include methods based on Link Quality [37] and Transmission Power Level [38], [39]. The remaining ones include TOA (Time of Arrival) [40] and 2.4 GHz Phase Thistle. The TOA method is based on measuring the time of propagation of radio waves between the transmitting device whose location is determined and the receivers installed in the Wi-Fi access points.

In order to achieve a high level of accuracy while using those methods (accuracy of 0.3 meters), it should be emphasized that a precise time synchronization is required between the transmitting and the receiving device, which is obtained

only by installing appropriate software in the device. It needs to be added that despite the use of advanced computational algorithms for ranging techniques, a number of limitations are encountered in practice that greatly affect the accuracy of positioning. Studies in [31], [41] have shown that RSS values, and thus the accuracy of positioning, greatly depend on the orientation (rotation) of the measuring device.

As explained above, the major advantage of passive measurements is that the device does not have to be aware of the communication (at the application level). This is the reason why the fingerprints technique relying on passive measurements is so popular. However, high accuracy of fingerprints depends on stable conditions, which are not easily achievable. One of the main drawbacks of this technique is that calibration and positioning are decoupled [42], [43], which results in different conditions under which the two processes are run, caused, for instance, by multi-device interference, changes in indoor furniture layout, etc. It must not be forgotten sources of error affecting this technique exist as well, such as shadowing channel effects [20], [44], or multipath effects [45], just to name a few. But at this particular time, we are going to focus on the first of the drawbacks mentioned above, since small changes in the environment result in a serious reduction of positioning efficiency [46]. Therefore, in this paper, we propose to combine calibration and positioning and dynamically adapt the fingerprints map during as the positioning system continues to operate.

The examples illustrating the technical advancement of existing solutions are results of a competition organized by Microsoft [47]. The main objective of the competition was to compare the results obtained with the use of different positioning technologies deployed inside buildings. 22 teams participated in this competition, representing both the academic community and the world of industry. From the technical point of view, different approaches were presented - from the deployment of a Wi-Fi network at existing premises, to the use of dedicated infrastructures, e.g. Bluetooth, magnetic resonators or ultrasonic transmitters.

The results of this competition can be regarded as a good benchmark for the existing solutions. It shows that the average positioning error rate that was achieved by the specific solutions ranged from 0.72 m to 10.22 m. Only 3 teams were able to achieve an accuracy of less than 2 m, while the accuracy of 3 m was achieved by half of all teams. In most cases, a significant increase in the share of faulty positioning results was observed when location/orientation of furniture changed. The 2017 IPIN Competition [48] is another occasion at which the existing solutions were presented. From all shown during this competition, only the AraraDS positioning system resembles our approach, but it is solely based on Wi-Fi. The remaining competitors used active location methods, as they requested information from the end device (accelerometer, magnetometer, gyroscope, compass, etc.).

III. Adaptive Indoor Positioning System

In this section, we provide implementation-related details of the location-based system for changing industrial environments. The system revolves around two main ideas:

(a) enhanced multi-technology multi-antenna hardware based on separation of network access and communication layers, and (b) an advanced fingerprints Machine Learning algorithm with system adaptation feedback, combining both calibration and positioning phases.

The requirements applicable to location-based systems operating in industrial environments are as follows:

- maximizing simplicity of the solution,
- minimizing the necessary investment,
- achieving positioning precision of less than 0.5 m,
- maximizing the number of technologies that may be used for localization purposes, in order to avoid interference.

With the above requirements taken into consideration, we designed a system based on the following assumptions:

- The activity at the premises would be monitored using the network available at the premises– WI-FI, RFID, IEEE 802.15.4, Bluetooth. Moreover, the system will be open to other, new technologies, meaning that the integration of these technologies will be as easy as possible. It is worth noting that the use of the RFID technology is legitimate in this context, as RFID systems operating in the 2.4 GHz band and using active tags (with their own power supply) are available, meaning that they can be used for monitoring purposes as well,
- The role of transceivers transmitting location signals must be performed by Industrial Internet of Things sensors,
- The role of a receiving device that collects and analyzes the location information must be performed by multi-technology controllers(at the under layer).

A. Multi-Technology Multi-Antenna Scenario Based on Separation of Network Access and Communication With Devices

The proposed positioning system is based on the measurement of the power of radio signal sent by the sensor of the monitored machine, using different 2.4 GHz band technologies, i.e. Wi-Fi, Bluetooth, RFID or IEEE 802.15.4 networks. It should be emphasized that while there are systems for localizing objects inside industrial premises using more than one technology, we are not aware of any solution (based on passive measurements) providing support for all the above-mentioned technologies.

Localization analysis based on measurements performed by sets of antennas shows a high positioning efficiency in indoor scenarios, but the most important inconvenience of using antenna arrays in the multi-technology approach is the extra price that this hardware carries with it. Each technology requires a number of antennas, each one with its own transceiver. Therefore, we provided a multi-technology antenna with a single physical transceiver, with its control being centralized and fully softwarized, as described in [49]. The softwarized platform ensures that all technologies use a single transceiver in TDD, which is a cost-saving solution. While designing this system, we used some of our previous ideas presented in [50]–[53].

The idea is to clearly separate network access and device communication functionalities. This means that multiple
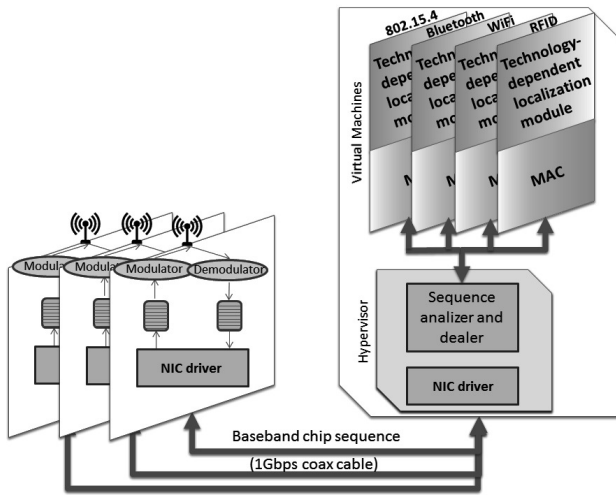
Fig. 1.   Multi-technology multi-antenna functional architecture.

protocols making up a part of the array module include simple hardware tasked with receiving beacons signals from the mobile devices and with forwarding them to the intelligence portion of the system. No other action is required on the part of the transceiver, which considerably reduces its cost and makes it possible to populate the analyzed space with a high number of small, single-transceiver modules performing a small number of functions.

The intelligence portion of the system considers all potential technologies and develops different virtualized nodes for managing device identification processes (based on different technologies) [54]. In our solution, we develop a virtualized software platform containing a number of nodes, with each one of them managing a different technology.

In the multi-technology multi-antenna solution presented in this paper, we introduced the most important 2,4 GHz technologies. Fig. 1 shows the operation of a multi-technology multi-antenna system. Its functioning is explicitly described in [50], with the technologies co-habiting via software. The use of a simple transmitter is sufficient to implement the solution. The radio portion will alternately perform the function of the devices operating in the abovementioned technologies (a time division will be applied). According to [55], the co-existence of many radio technologies depends on three factors: frequency, location in space and time. If the individual radio networks differ at least with regard to one of the aforementioned factors, they will be able to function properly. In our case, as we use the same transceivers (which means the same frequency and location), coexistence of multiple technologies may only be achieved through the introduction of a time-division. The two main advantages of this solution are the lack of interference between different technology devices (since the transceiver kit performs the function of one technology only during a certain period of time, it does not affect the accuracy of device positioning by generating interference).

Wi-Fi and 802.15.4 transceivers perform a few functionalities related to signal demodulation and to transmission of digital information to the central virtualized platform that will address the digital information to the appropriate virtual machine, depending on the technology used.

Wi-Fi transceivers contain the Physical Medium Dependent (PMD) layer only, responsible of converting electrical signals into arrays of bits. Different encoding techniques may be used here (including, inter alia, DBPSK, DQPSK, BPSK, QPSK, CCK, QAM), depending on the version of the standard used and the distance between the mobile device and the transceivers. The encoding technique (and modulation) used defines the maximum bitrate in each channel and, in consequence, the bitrate necessary to transport information from the transceiver to the platform.

From the point of view of 802.15.4, the transceivers only manage the baseband chip sequence at the physical layer. The chip sequence is a direct mapping of raw data into a set of ones and zeros that are afterwards modulated by the electrical signal (half-sine pulse factor used in offset quadrature phase-shift keying, O-QPSK). In our solution, this sequence is sent directly from the transceiver to the platform, where the sequence is converted into raw data. The baseband chip sequence contains the same information as raw data but requires a higher bitrate due to the high overhead introduced by the physical layer, which limits the transmission capacity between the transceiver and the platform, while simultaneously reducing complexity of the modules. In fact, the baseband chip sequence includes the PHY Protocol Data Unit (PPDU) for synchronizing the signal within the receptor, as well as additional information, e.g., frame length. The baseband chip sequence contains more than eight times more bits than raw data, since each 4 bits of raw data are encoded in 32 chip values and, in addition, PPDU is added.

The platform contains higher layer functionalities of the considered technologies. When relying on Wi-Fi, the platform assumes the functionalities of the Physical Layer Convergence Procedure (PLCP) that is responsible for analyzing the preamble and PHY headers, and the functionalities of layer 2 and layer 3. In fact, the transceiver continuously sends demodulated bits, but it does not interpret the sequence of bits. Upon receiving the bit sequence, the platform analyzes that sequence and extracts information related to the entire transmission (starting from the understanding of the bounds of the transmission in the sequence of bits based on the location of the preamble).

The platform responsible for managing the technologies is based on a virtualized machine, where each Virtual Machine (VM) hosts one of the technologies. The hypervisor is in charge of controlling the functioning of the VMs, as well as for managing communication with the network adapter. The frames arriving from NIC (Network Interface Card) are copied in all VMs, irrespective of the technology of the frame. The VM is in charge of discarding/accepting the frame if it is/is not compatible with the technology of the VM. The MAC layer has been implemented in all technologies, taking decisions about discarding/accepting specific frames.

In addition to MAC functionalities, each VM operates as a positioning module. These modules are responsible for executing the positioning process, which is technology-dependent (fingerprints are different for each of the technologies). Let us remark that technology-dependence is a factor affecting all technologies, which makes the implementation process easier.

To recapitulate - the proposed modulated system is based on softwarization of the primary (device) communication functionalities – a solution that is possible thanks to the reduced communication load (based on beacons only) required in the indoor positioning system, and allows to reduce CAPEX and OPEX thanks to the simplicity of the radio system. The result is a cost-saving multi-antenna and flexible (softwarization) multi-technology system that may be easily adapted to any harsh industrial scenario. Currently, the price of hardware for the presented solution is in the tens of thousand of euro range, making the complete solution an affordable investment in practically any industrial environment.

B. Fingerprints Based on the Machine Learning Algorithm

We introduced fingerprints that are based on Machine Learning, meaning that the algorithm creating the fingerprints map is continuously learning the environment. Our method uses passive measurements based on beacons sent by the sensors. From such signals, the receivers measure RSS and, based thereon, location of the devices is estimated.

In the traditional two-phase approach to fingerprints, a test device is initially positioned at many physical locations (a grid of physical points) of the testbed. The device is connected and RSS of the signal received from the device (for each message within the connection setup) is measured at the transceiver (this process is referred to as calibration). The map of all RSS measurements serves as a basis for positioning the devices, i.e. for the second stage of the process (referred to as localization). The change in the conditions occurring between the two processes (calibration and localization) is the main disadvantage of such an approach; a situation in which obstacles are introduced (e.g. factory workers) during the localization process, not present at the map building stage (calibration), is a good example here.

Therefore, we propose a fingerprints methodology that learns about the environment in a continuous manner. Machine learning is achieved thanks to a high number of RSS measurements taken during the whole lifecycle of the system at the specific industrial premises, so these measurements provide feedback about the electromagnetic environment during the communication process.

In our solution, the calibration process is divided into two stages. The first one occurs "off-line", i.e. when no activities take place at the factory. These measurements are very precise and the process is slow due to numerous repetitions during which good samples are collected. The second phase of the calibration process is performed during the positioning stage (and is known as "on-line" calibration), when the factory operates normally. Several testing devices are located throughout the premises and they operate jointly with the sensors that need to be localized, which provokes interference, echoes, obstacle effects, etc. The test devices continuously provide feedback about the environment. On-line calibration measurements are interpolated into their off-line counterparts in order to obtain the final fingerprints map.

In the localization process, the sensors (to be localized) are positioned at a given point of the analyzed space by comparing
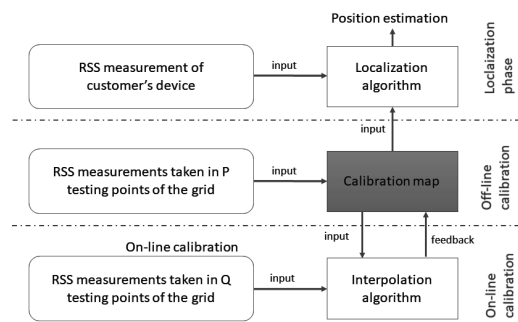

Fig. 2. Phases of the proposed fingerprints localization method.

the signal arriving from the sensor with the final fingerprints map. Statistical tools are used for obtaining the position with the highest degree of accuracy possible.

The diagram of the entire process is presented in Fig. 2.

1) Off-Line Calibration: Off-line calibration is the classic calibration performed as part of the fingerprints method.

Estimation of fingerprints consists in taking statistically significant RSS measurements from all test points within the analyzed area. The minimum distance between two neighboring test points is lower-bounded by the positioning accuracy required by the manufacturing application, as well as by the limits applicable to hardware and statistical tools. Details concerning the minimum distance are discussed in the following sub-section. For the moment, let us assume that we have, in off-line calibration, P test points located throughout the analyzed surface.

A test device sends an identifiable data sample and RSS of the signal arriving at, say N transceivers, is measured. The test device repeats this operation in order to obtain a number (say M) of RSS measurements at the transceivers, so that a consistent average may be obtained. The off-line calibration map contains N-dimensional mean values (of M measurements) for each testing point, along with the physical location of the test point.

2) On-Line Calibration: Q test devices, which are fixed devices that emit signals periodically, are located throughout the analyzed area, so that on-line calibration is performed with Q test points whose number is lower than that of P test points in off-line calibration. Each of the Q test devices sends beacon request samples in intervals. Based on RSS measurements related to these signals, the calibration map is recalculated by using an interpolation algorithm (see Fig. 2). This algorithm takes the old calibration map values and updates them by introducing information from the new RSS measurements, in the manner described below.

For the purpose of the algorithm, fingerprints values are taken only based on the most recent M samples, whereas the previous samples are discarded. This signal is received at all N transceivers and RSS is measured. Let $RSS_{m,n}^{\overrightarrow{x_q}}$ be the RSS value of the signal emitted by the test device located at $\overrightarrow{x_q}$, $(q = 1..Q)$ at a time equal to the current timer: $(M - m) \times \tau$, $(m = 1..M)$, and measured in transceiver n, $(n = 1..N)$.

Due to the changing environmental conditions, the last (time-wise) calibration measurements are likely to be more precise than their predecessors, as the former have been taken in conditions that are much more similar to the current conditions (compared to previous measurements). Therefore, we introduce a moving average of the calibrated measurements for updating the calibration map. We consider Weighted Moving Average (WMA) and Exponential Moving Average (EMA) of the new RSS (from Q-test devices) measurements. Suitability of the moving average depends on the scenario and, specifically, on the impact the environment exerts on the measurements during measuring interval τ. If the environment is affected by numerous changes that rapidly change the measurement values, then EMA should be used, otherwise WMA will be appropriate. So, in principle, for very harsh manufacturing environments, EMA is better than WMA.

Let $\left[\overline{WMA^{\vec{x_q}}}\right]$ and $\left[\overline{EMA^{\vec{x_q}}}\right]$ be the vectors of Weighted Moving Averages and Exponential Moving Averages of RSS measurements arriving from a test device located at $\vec{x_q}$:

$$\left[\overline{WMA^{\vec{x_q}}}\right] = \left[\begin{array}{c} \dfrac{\sum_{m=0}^{M-1}(M-m) \times RSS^{\vec{x_q}}_{(M-m),1}}{M \times \frac{M+1}{2}} \\ \dfrac{\sum_{m=0}^{M-1}(M-m) \times RSS^{\vec{x_q}}_{(M-m),2}}{M \times \frac{M+1}{2}} \\ \vdots \\ \dfrac{\sum_{m=0}^{M-1}(M-m) \times RSS^{\vec{x_q}}_{(M-m),N}}{M \times \frac{M+1}{2}} \end{array}\right]$$

$$\left[\overline{EMA^{\vec{x_q}}}\right] = \left[\begin{array}{c} \alpha \times \sum_{m=1}^{M}(1-\alpha)^{M-m} \times RSS^{\vec{x_q}}_{m,1} \\ \alpha \times \sum_{m=1}^{M}(1-\alpha)^{M-m} \times RSS^{\vec{x_q}}_{m,2} \\ \vdots \\ \alpha \times \sum_{m=1}^{M}(1-\alpha)^{M-m} \times RSS^{\vec{x_q}}_{m,N} \end{array}\right]$$

$$with \ \alpha = 1 - 0.05^M \tag{1}$$

The value $\alpha = 1 - 0.05^M$ ensures that the sum of the weights of the M last samples equals 95% of all the measurement samples recorded. With RSS values of the on-line test points, we may estimate the RSS values of other (P-Q) test points within the investigated area (these P-Q test points were present in off-line, but not in on-line calibration. However they are a part of the calibration map). For estimating RSS values of $\vec{x_p}$, $(p = 1..P)$ (say $RSS^{\vec{x_p}*}$), we scale the off-line fingerprints values $RSS^{\vec{x_p}}$ by observing the scaling trend of the (physically) nearest on-line test points. In other words, by observing how RSS varies at the on-line test points, we can estimate how much RSS changes at off-line test points. This methodology assumes that close test points behave similarly to environmental changes (e.g. a new obstacle in the room). For the purpose of estimating RSS values of P points, we perform an interpolation of the Q nearest on-line test points (see Fig. 3).

For each measurement of on-line test devices, we estimate the RSS values at P-Q off-line points together with moving average values ($\left[\overline{WMA^{\vec{x_q}}}\right]$ or $\left[\overline{EMA^{\vec{x_q}}}\right]$) of the off-line
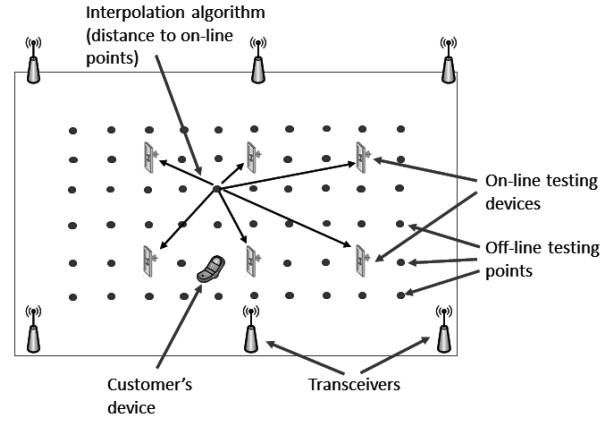

Fig. 3. Example of an indoor localization scenario ($N = 6$; $P = 60$; $Q = 6$).

points. Specifically, the estimation of RSS for testing point $\vec{x_p}$, i.e. $RSS^{\vec{x_p}*}$, considers the relation of averages between itself and each on-line test point, so:

$$RSS^{\vec{x_p}*} \alpha \frac{\overline{MA^{\vec{x_p}}}}{\overline{MA^{\vec{x_q}}}}, \tag{2}$$

where $\overline{MA^{\vec{x_p}}}$ is any of the moving averages' vectors ($\left[\overline{WMA^{\vec{x_p}}}\right]$ or $\left[\overline{EMA^{\vec{x_p}}}\right]$).

Moreover, as stated above, the interpolation formula considers that an off-line point suffers similar variations as the on-line test points that are close to it (the closer, the more similar the variations become). In order to understand the effect of proximity of on-line points, let us remark that RSS decreases proportionally to the square of the distance from the test device, as is described in the well-known Friis transmission equation. Therefore, we consider that:

$$RSS^{\vec{x_p}*} \alpha \frac{1}{(d^{\vec{x_p}\vec{x_q}})^2}, \tag{3}$$

where $d^{\vec{x_p}\vec{x_q}}$ is the Euclidean physical distance (in meters) between the off-line test point to be estimated ($\vec{x_p}$) and each one of the on-line test points ($\vec{x_q}$).

So, $RSS^{\vec{x_p}*}$ is estimated from the values $RSS^{\vec{x_q}}$ by using the following interpolation formula:

$$RSS^{\vec{x_p}*} = \sum_{i=1}^{Q} \left[\frac{1}{Q} \times RSS^{\vec{x_i}} \times \frac{\overline{MA^{\vec{x_p}}}}{\overline{MA^{\vec{x_i}}}} \times \frac{\sum_{j=1}^{Q}(d^{\vec{x_p}\vec{x_j}})^2}{(d^{\vec{x_p}\vec{x_i}})^2} \right], \tag{4}$$

where terms $\frac{1}{Q}$ and $\sum_{j=1}^{Q}(d^{\vec{x_p}\vec{x_j}})^2$ are normalizing factors. The normalizing factor $\frac{1}{Q}$ averages out the effect of Q measurements (from off-line point p to each one of the Q on-line points), whereas factor $\sum_{j=1}^{Q}(d^{\vec{x_p}\vec{x_j}})^2$ introduces information about the distance between p and each one of the Q on-line points.

Let us remark that formula (4) is our proposal related to interpolation, but it is not unique. Many other interpolation formulas may be found in literature, but the one presented here is the simplest one that takes into account the effect of distance in Q measurements.

The value of $RSS^{\overrightarrow{x_p}*}$ is estimated for each new measurement of on-line test devices. So, when a new estimation is calculated, then we can also calculate the moving average values ($\left[\overline{WMA^{\overrightarrow{x_p}}}\right]$ or $\left[\overline{EMA^{\overrightarrow{x_p}}}\right]$) of P-Q off-line points, from the last M estimated values of $RSS^{\overrightarrow{x_p}*}$, as indicated in (1). This average ($\left[\overline{WMA^{\overrightarrow{x_p}}}\right]$ or $\left[\overline{EMA^{\overrightarrow{x_p}}}\right]$) is used in formula (4).

As a result of the abovementioned operations, we obtain a full fingerprints map, with measurements and estimations performed in the real operating conditions. The map considers interference, signal shadowing and other effects caused by other machines present within the area under analysis.

The process of updating the map requires considerable processing power, since large amounts of data are processed in each time interval τ. The same will be the case with the localization process. However, the latter will be run only when device signal is received by the transceivers.

3) Device Positioning: Once the fingerprints map is ready, the device (e.g. a machine) may be positioned within the analyzed space by comparing its RSS (arriving at the transceivers) with the calibrated fingerprints map. Let $\left[RSS^d\right]$ be the N-vector of RSS values of the signal arriving from the device to be localized, d.

In order to estimate the location of the device, we calculate the Mahalanobis distance, dM_pd, between RSS^d and each one of the P vectors $\left[\overline{WMA^{\overrightarrow{x_p}}}\right]$ or $\left[\overline{EMA^{\overrightarrow{x_p}}}\right]$, $p = 1..P$ obtained from P test points, as indicated in (5). The location of the device to be localized will be the same as that of test device p', $p' \in [1, P]$, whose Mahalanobis distance $dM_{p'd}$ is minor. The Mahalanobis distance takes into account not only the N-dimensional distance between two N-dimensional measurements, but also the variance that the measurements suffer in each one of the N dimensions. In our case, the Mahalanobis distance takes into account the variance of the different measurement points (transceivers), because those with high variability of RSS measurements are considered to be exposed

to uncertainty, meaning that this distance also takes into account which transceivers provide more (secure) information for localizing a given point.

The Mahalanobis distance is calculated as follows:

$$dM_{pd} = \sqrt{\left(\left[RSS^d\right] - \overline{MA^{\overrightarrow{x_p}}}\right)^T} \times \sqrt{\left[CoV^{\overrightarrow{x_p}}\right]^{-1} \times \left(\left[RSS^d\right] - \overline{MA^{\overrightarrow{x_p}}}\right)}, \quad (5)$$

where $\overline{MA^{\overrightarrow{x_p}}}[i]$ is the i-element of any of the moving average vectors: $\left[\overline{WMA^{\overrightarrow{x_p}}}\right]$ or $\left[\overline{EMA^{\overrightarrow{x_p}}}\right]$, and $\left[CoV^{\overrightarrow{x_p}}\right]$ is the covariance matrix, which is calculated with the last M RSS values of all P test points. $\left[CoV^{\overrightarrow{x_p}}\right]$ is formulated in (6), as shown at the bottom of this page.

The co-variance matrix computes the correlation between the RSS samples measured at the transceivers, so that the matrix shows how uniform the samples arriving at each module are.

4) Discussion Concerning Assumptions: The efficiency of the system may be restricted by hardware and software limitations, and by variability of the environment. Hardware limitations affect measurement accuracy, influencing the minimum physical distance that may be distinguished by the system. As far as software is concerned, even with such considerable amounts of data being processed, the tests failed to identify any issues related to data processing, meaning that the software relied upon is good enough to process the data arriving from test points and from devices located throughout the manufacturing premises.

Finally, high variability of the environmental conditions could require an adjustable sampling rate of probes during the on-line calibration stage.

Hardware limitations affecting the minimum distance between test points and the frequency of on-line calibration probing will be described below.

5) Defining the Distance Between Test Points: Precision of the off-line calibration map depends on the transceivers' ability to distinguish two test devices which are located close

$$\left[CoV^{\overrightarrow{x_p}}\right]$$

$$= \frac{1}{M-1} \times \begin{bmatrix} \sum_{m=1}^{M}(RSS_{m,1}^{\overrightarrow{x_q}} - \overline{MA^{\overrightarrow{x_p}}}[1])^2 & \sum_{m=1}^{M}(RSS_{m,1}^{\overrightarrow{x_q}} - \overline{MA^{\overrightarrow{x_p}}}[1]) \times \\ & \times (RSS_{m,2}^{\overrightarrow{x_q}} - \overline{MA^{\overrightarrow{x_p}}}[2]) & \cdots & \sum_{m=1}^{M}(RSS_{m,1}^{\overrightarrow{x_q}} - \overline{MA^{\overrightarrow{x_p}}}[1]) \times \\ & & & \times (RSS_{m,N}^{\overrightarrow{x_q}} - \overline{MA^{\overrightarrow{x_p}}}[N]) \\ \sum_{m=1}^{M}(RSS_{m,2}^{\overrightarrow{x_q}} - \overline{MA^{\overrightarrow{x_p}}}[2]) \times & \sum_{m=1}^{M}(RSS_{m,2}^{\overrightarrow{x_q}} - \overline{MA^{\overrightarrow{x_p}}}[2])^2 & \cdots & \sum_{m=1}^{M}(RSS_{m,2}^{\overrightarrow{x_q}} - \overline{MA^{\overrightarrow{x_p}}}[2]) \times \\ \times (RSS_{m,1}^{\overrightarrow{x_q}} - \overline{MA^{\overrightarrow{x_p}}}[1]) & & & \times (RSS_{m,N}^{\overrightarrow{x_q}} - \overline{MA^{\overrightarrow{x_p}}}[N]) \\ \vdots & \vdots & \vdots & \vdots \\ \sum_{m=1}^{M}(RSS_{m,N}^{\overrightarrow{x_q}} - \overline{MA^{\overrightarrow{x_p}}}[N]) \times & \sum_{m=1}^{M}(RSS_{m,N}^{\overrightarrow{x_q}} - \overline{MA^{\overrightarrow{x_p}}}[N]) \times & \cdots & \sum_{m=1}^{M}(RSS_{m,N}^{\overrightarrow{x_q}} - \overline{MA^{\overrightarrow{x_p}}}[N])^2 \\ \times (RSS_{m,1}^{\overrightarrow{x_q}} - \overline{MA^{\overrightarrow{x_p}}}[1]) & \times (RSS_{m,2}^{\overrightarrow{x_q}} - \overline{MA^{\overrightarrow{x_p}}}[2]) & & \end{bmatrix}$$

$$(6)$$

to other. The range of the transceivers is limited by the physical layout of the space under analysis, by hardware limitations, power-consumption limitations (power of the signal) and by other factors. In general, there is a trade-off between accuracy and cost levels, as better accuracy may be achieved only by increasing costs (better hardware, more powerful signal, longer calibration process due to a higher number of test points, etc.). The other precision-affecting restriction has the form of the requirements that the industrial application relying on the location-based service has to satisfy. In a specific application, a lower positioning accuracy than the one offered by the system may be needed, for instance. In this case, it makes no sense to invest in a very precise calibration map.

Where accuracy is limited by the system's capabilities, a minimum distance between test points needs to be established (accuracy of the calibration map) that can be properly measured by the transceivers. Therefore, we analyze RSS (measured at the transceivers) of the signals originating from two neighboring test devices, and check whether they are statistically different. In this context, the first step of the off-line calibration process is to measure RSS of the signal arriving from test devices situated at two (physically) close points $\overrightarrow{x_p}$ and $\overrightarrow{x_q}$. The test is repeated several times (say M) for each of the points. Let $RSS_{m,n}^{\overrightarrow{x_p}}$ and $RSS_{m,n}^{\overrightarrow{x_q}}$, m = 1..M, n = 1..N, be the RSS measurements from test points $\overrightarrow{x_p}$ and $\overrightarrow{x_q}$, respectively.

We consider that $\overrightarrow{x_p}$ and $\overrightarrow{x_q}$ are statistically distinguishable if any averages or the variance between $RSS_{m,n}^{\overrightarrow{x_p}}$ and $RSS_{m,n}^{\overrightarrow{x_q}}$ are different. This is because while performing the device positioning process, the system will use Mahalanobis distance, considering both average and variance (note that the Mahalanobis distance between the measurements of the device and the two calibration points, dM_{pd} and dM_{qd} will be different if average or variance are different). Thus, it is possible that the device is properly localized even if the averages of $RSS_{m,n}^{\overrightarrow{x_p}}$ and $RSS_{m,n}^{\overrightarrow{x_q}}$ are equal, with variances being the only different factors. Fig. 4 shows an example of a scenario in which the blue and red points are the averages of $RSS_{m,n}^{\overrightarrow{x_p}}$ and $RSS_{m,n}^{\overrightarrow{x_q}}$, respectively, whereas the ellipses represent the increasing Mahalanobis distance from the averages. If a device is located at a given point (whose RSS measurement is represented by the black point), then the device should be clearly localized at $\overrightarrow{x_q}$ despite its RSS being closer to the average of test point $\overrightarrow{x_p}$.

In order to calculate whether $\overrightarrow{x_p}$ and $\overrightarrow{x_q}$ are statistically different, the first step is to compare variances of ($\overrightarrow{x_p}$ and $\overrightarrow{x_q}$) test measurements. Variances are compared separately for each one of the N (assumed normal) measurement sets, meaning that two test points will be considered being statistically different if the RSS samples measured at any transceiver coming from $\overrightarrow{x_p}$ and $\overrightarrow{x_q}$ are not equal for a given significance level (90%). We use the Cochran test and compare the results with applicable tables to determine whether the 90%-significance level has been achieved.

If all variances are equal, then we compare the averages by using the MANOVA test. The MANOVA tests uses any of the statistics existing for comparing the means; in our case we will use the Hotelling T-squared statistic and will
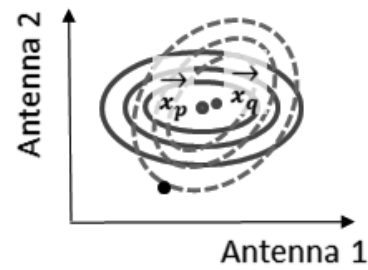

Fig. 4. Example of Mahalanobis distance for two neighboring points.

compare with F-distribution values, which allows us to reject (or not) the null hypothesis that the averages are equal (at a required significance level). We selected the Hotelling T^2 statistic, because it describes the behavior of the Mahalanobis distance between the averages of two groups ($\overrightarrow{x_p}$ and $\overrightarrow{x_q}$) and compares this distance with the tabulated values. It was already mentioned previously why Mahalanobis distance is better at describing the incidence of transceivers into the measurements.

Let us remark that the statistical tools used here require significant amounts of data in order to compare variances and averages – a requirement that may be satisfied only by conducting a long testing process. Here, proper balance between the necessary positioning accuracy and testing process costs should be ensured. In our tests, the results showed that in an area of 100 m^2 scanned by six transceivers, the minimum distance of 40 cm may be achieved.

6) On-Line Calibration Sampling Rate: Whereas off-line calibration measures the effect of stable conditions (furniture, transceivers, etc.) on the calibration map, on-line calibration estimates the effect of changing conditions. The latter are more difficult to estimate and an adequate measurement frequency relied upon during on-line calibration is crucial in order to properly calculate the calibration map: measurements that are too sporadic could lead to a conclusion that older measurements provide false information about the condition of the space under analysis (e.g. old measurements provide information about the impact exerted by other machines that are no longer present at the same location in the room), and could result in a false calibration map being drawn up. On the other hand, too frequent measurements could make the measurements excessively uniform, which would eliminate important information concerning reliability of transceivers (determining the degree of precision of each transceiver).

Therefore, we introduce a mechanism for adjusting the sampling rate of the on-line calibration measurements to ensure that probing is not too frequent or too sporadic. Let us consider M last on-line calibration measurements forming a time series. The objective is that the time series is not a purely stationary process (caused by the same environmental conditions prevailing throughout the entire measurement period, meaning that the measurements are too frequent and all of them render the same results), and, at the same time, it contains a non-jerky deterministic component (a jerky series is caused by suddenly changing conditions, indicating that old measurements are not depicting the current state of the environment anymore). Therefore, a non-stationary series with

a non-jerky deterministic component ensures that the time series picks up the changes in the environment, simultaneously avoiding the registration of sudden changes.

We split the time series into K periods (K groups of samples), so that each period contains M/K measurement samples. The value of K should be as high as possible, simultaneously ensuring that M/K is high enough to obtain the expected values (mean and variance) with sufficient statistical significance. First, we check that the series is not stationary-like and, afterwards, that it is not jerky:

We consider that the time series is stationary if each one of the K groups has the same average. For this purpose, we apply the ANOVA method which uses the variance of the groups in order to understand whether the differences between the averages are caused by variations inside the group, or by differences between groups. where the averages differ significantly (significance level of 90%, i.e. the value in the F-distribution is $F_{0.9,K-1,M-K}$), then the probing frequency is maintained. Otherwise, the probing frequency is reduced in steps of 10% of its current value.

The series is jerky when there are appreciable differences between consecutive groups of samples. Therefore, in order to investigate the jerky character of the time series, mean values of each group of samples ($\overline{RSS_{k,n}^{\overrightarrow{x_p}}}$) are calculated:

$$\overline{RSS_{k,n}^{\overrightarrow{x_p}}} = \frac{K}{M} \times \sum_{i=k\times\frac{M}{K}+1}^{(k+1)\times\frac{M}{K}} RSS_{i,n}^{\overrightarrow{x_p}}, \quad k = 1..K-1, \ n = 1..N$$

(7)

Afterwards, we calculate the difference:

$$\left| \overline{RSS_{k+1,n}^{\overrightarrow{x_p}}} - \overline{RSS_{k,n}^{\overrightarrow{x_p}}} \right|, \quad where \ k = 1..K-1, \ n = 1..N$$

(8)

and compare each value with the average $\sum_{i=2}^{M} \frac{\left| RSS_{i,n}^{\overrightarrow{x_p}} - RSS_{i-1,n}^{\overrightarrow{x_p}} \right|}{M-1}$, $n = 1..N$. Notice that we compare the jumps between the groups with the mean jump value between consecutive samples in the entire series. This is because we are searching for jerky behavior between groups and not between single samples, but the differences between samples offer information about the "acceptable" values of the jumps. Where any value $\overline{RSS_{k,n}^{\overrightarrow{x_p}}}$, $k = 1..K-1, \ n = 1..N$ fulfills formula (9) for any of N transceivers, the sampling rate is increased by 10%. Otherwise, it is maintained without any modifications.

$$\left| \overline{RSS_{k+1,n}^{\overrightarrow{x_p}}} - \overline{RSS_{k,n}^{\overrightarrow{x_p}}} \right| > U \times \sum_{i=2}^{M} \frac{\left| \overline{RSS_{i,n}^{\overrightarrow{x_p}}} - \overline{RSS_{i-1,n}^{\overrightarrow{x_p}}} \right|}{M-1} \quad (9)$$

Let us remark that U is a set-up parameter that depends on the space under analysis. In order to calculate a proper U value, an experiment should be conducted at the beginning of the system's lifecycle: a test device situated at $\overrightarrow{x_p}$ sends signals under stable (stationary) and changing conditions. The value of U should be such that it allows to understand whether the value

$\left| \overline{RSS_{k+1,n}^{\overrightarrow{x_p}}} - \overline{RSS_{k,n}^{\overrightarrow{x_p}}} \right|$ is caused by the stationary or changing nature of the conditions prevailing in the test environment.

The mechanism for checking and adjusting the sampling rate is applied when M new probes are measured at the transceivers. In this way the operations described previously are always based on different $RSS_{m,n}^{\overrightarrow{x_p}}$ values. Sampling rate adjustment does not have to be a real-time process, so adjustments performed in $M \times \tau$ time intervals seem to be quite appropriate. Adjustment of the sampling rate requires a communication framework between the system and the test devices in order to inform the period length. However, this capability has not been developed yet in our system (future work). Sampling rate adjustment offers energy savings, as the test devices situated at $\overrightarrow{x_p}, \ p = 1..P$ may go to sleep during, and may only operate when necessary. This functionality has not been developed in our current implementation as well.

IV. TESTBED EXPERIMENTS

We adopted the following test parameters: (1) only one device is tracked, its position is well-known, so that the difference between the actual and estimated position (provided by the system) may be calculated. In the test, the device has the form of a chipset sending beacons. However, in real industrial applications, the devices that need to be localized are industrial machines or sensors attached to mobile machines, or mobile phones owned by maintenance workers or any other mobile hardware with a radio communications interface. The process of locating a single device is performed for the purpose of the test only, although the system is capable of localizing numerous devices (machines or workers' mobile phone) simultaneously. However, it would be very difficult to prove the efficiency of the system by conducting tests measuring the signal of the devices (without any knowledge about the precise condition of those devices); (2) even though the modules used are of the multi-technology variety, for the purpose of these tests, the device to be localized communicates uniquely via Bluetooth. We selected the Bluetooth technology because it has been demonstrated that, in regards to indoor positioning, Bluetooth is less efficient than WiFi [56]–[58]. As a conclusion, if the test results show that our system, relying on Bluetooth, is more precise than current solutions, then we can conclude that our system operating based on WiFi will achieve even better results, or at least ones that are not worse. Some tests are performed during normal operation of the factory, with numerous IIoT generating interference, signal shadows and serving as obstacles.

The system has been implemented and tested in and indoor scenario (a room with the area of 100 square meters and volume of 400 cubic meters). The tests included functional and performance trials: in the functional tests we analyze the parameters of the model (calibration phases) and, specifically, the minimum distance between test points, off-line accuracy in a multi-antenna environment, on-line calibration setup parameters and the impact of the moving average on the results obtained with the use of the algorithm. In the performance tests, we compare the functioning of our system with the same system that does not include the on-line calibration phase.

This test allows us to compare the system with other solutions that have been proposed so far.

A. Off-Line Calibration - Minimum Distance Between Test Devices

This test aims to determine the minimum distance between test devices, such that the system may distinguish the signals arriving from neighboring test points. The minimum distance is indicated by points on the calibration map. This distance does not necessarily define the degree of precision of the system, but it is precision-related. In other words, even if the calibration map has specific points which are separated by the minimum distance, other factors, such as obstacles, interference, etc. may render that location of devices at their accurate positions on the map not achievable. Let us remark that this minimum distance is related to the value obtained in the tests described in [47], meaning that this distance may be used for comparison (taking into account the differences in the scenario) with the solution proposed there.

The test scenario is as follows: the surface contains 6 transceivers located within the perimeter. The device to be localized is located in the center of the room and RSS is measured 100 times at the transceivers ($RSS_{m,n}^{\overrightarrow{x_p}}$, $m = 1..100$, $n = 1..6$). Then, the device is located on the horizontal axis (spanning the room west-east), at distances equal to 0.2, 0.4, 0.6, 0.8 and 1.0 m of $\overrightarrow{x_p}$ and RSS is measured 100 times at all transceivers, i.e.:

$$RSS_{m,n}^{\overrightarrow{x_q}}, \ \overrightarrow{x_q} = \overrightarrow{x_q} + x, \quad x = [0.2, 0.4, 0.6, 0.8, 1.0],$$
$$m = 1..100, \ n = 1..6 \quad (10)$$

$RSS_{m,n}^{\overrightarrow{x_q}}$ values are compared with $RSS_{m,n}^{\overrightarrow{x_p}}$ through Cochran and MANOVA tests. The Cochran test (Cochran's C test) showed that the measurement variances at all transceivers were similar, since the C values obtained from the measurements were much higher than the critical value of 0.23 obtained from the tables (6 variables and 100 samples), meaning that homoscedasticity is confirmed. Therefore, we used MANOVA for comparing the mean of the $RSS_{m,n}^{\overrightarrow{x_p}}$ values with each one of the means of $RSS_{m,n}^{\overrightarrow{x_q}}$ values. The Hotelling T^2 value of the test was compared with the F-distribution table (F = 2.72 for 6-numerator and 193-denominator freedom degrees and 0.9-significance level) for each one of the test points $\overrightarrow{x_q}$. The results are presented in Fig. 5.

As we can see, for a significance interval equal to 0.9, the minimum distance between test points is 0.4 m. For the distance of 0.2 m, RSS measured from devices located at $\overrightarrow{x_p}$ and $\overrightarrow{x_q}$ is not distinguishable, so the system is not capable of localizing a device at one of these two points.

There are some considerations concerning these results. As mentioned above, the figure of 0.4 m does not determine the degree of precision of the system, as there are other factors which may affect precision in an adverse manner. One sample from our test, which measured the device located at $\overrightarrow{x_p}$ +0.4 m in our test, is a good example here. RSS values measured (at all transceivers) were very similar to the mean $RSS^{\overrightarrow{x_p}}$ value, which indicates that in regards to that measurement, the positioning of the device would be erroneous. For all other
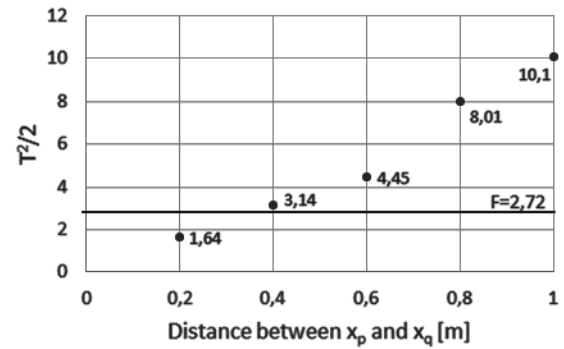

Fig. 5. MANOVA results for increasing distance between $\overrightarrow{x_p}$ and $\overrightarrow{x_q}$.

measurements, the positioning would be correct. However, this case shows that other factors exist limiting the efficiency of the system.

Once the minimum distance was defined as equaling 0.4 m, we performed similar tests by locating the test device at locations along a 0.4-squared grid and generated an off-line calibration map. This map was then used in further tests.

B. Off-Line Positioning Efficiency

The following test aims to show the impact of the number of transceivers on the system's positioning accuracy. Specifically, we situated the test device at many (500) known locations within the room and took measurements of the signal at N (N = 3, 4, 5 and 6 transceivers). Based on these measurements, the system made a localization decision by comparing the measurements with the appropriate off-line calibration map (4 calibration maps were built based on off-line measurements taken by 3, 4, 5 and 6 transceivers).

The difference between the actual and estimated position (absolute value of 500 measurements), obtained with a different numbers of transceivers, is presented in Fig. 6. The figure shows that the mean positioning accuracy of the measurements is on the 0.95-percentile (the upper bound of the positioning error of the 95% most precise measurements). The 0.95-percentile provides some information for estimating whether the variations observed in the mean values are statistically significant. Clearly, the (statistical) significance of the variations of the averages cannot be demonstrated with so few measurements, but the 0.95-percentile offers a better understanding of the significance.

The system localizes the device at one of the points of the 0.4-square grid calibration map, so the decision should be considered correct if the selected point on the map is the closest to the actual location of the device. Therefore, differences of less than 0.2 m indicate a correct decision, with differences higher than $0.2\sqrt{2}$ being always incorrect. Between 0.2 and $0.2\sqrt{2}$, the correctness of the decision depends on the position of the device (i.e. whether the localized position is the same as the closest map point).

In the case of 4 transceivers measuring the signals, the mean value of the differences between estimated and actual device location is lower than 0.2. Nevertheless, there are many incorrect decisions, as evidenced by the 0.95-percentile value

TABLE I

VALUES FOR ON-LINE CALIBRATION SAMPLING RATE TESTING

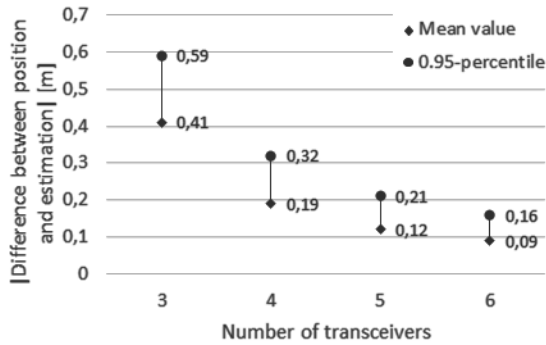| On-line sampling rate [samples/min.]	F_{exp}	$F_{0.9,3,196}$	Should sampling be decreased?	$max\left|\overline{RSS_{q+1,n}^{\overrightarrow{x_p}}} - \overline{RSS_{q,n}^{\overrightarrow{x_p}}}\right|$ [dbm]	$\frac{3}{M-1} \times \sum\limits_{i=2}^{M}\left|\overline{RSS_{i,n}^{\overrightarrow{x_p}}} - \overline{RSS_{i-1,n}^{\overrightarrow{x_p}}}\right|$	Should sampling be increased?
40	9.40±2.21	5.14	No	3.31	2.26	Yes
60	8.80±2.01	5.14	No	2.28	2.27	Yes
80	7.86±4.12	5.14	No	2.24	2.25	No
100	7.01±4.51	5.14	No	2.17	2.22	No
120	6.24±1.32	5.14	No	2.15	2.19	No
140	5.24±1.39	5.14	No	2.14	2.20	No
160	5.18±3.88	5.14	No	2.14	2.16	No
180	4.74±1.17	5.14	Yes	2.12	2.15	No
200	4.01±1.00	5.14	Yes	2.13	2.12	No

Fig. 6.   Positioning accuracy vs. number of transceivers.

equal to $0.32 > 0.2\sqrt{2}$. Only with five and six transceivers measuring RSS, the results show 100% correct positioning decisions. The achievement of this perfect localization is explained by the fact that there is only one device in the room, so no interferences are present and, in addition to this, the factory furniture has not been moved and remained at the same position as during off-line calibration, meaning that the map is perfect match for the actual test scenario.

The conclusion from these tests is that a high number of transceivers in a small room is needed to implement a high efficiency positioning system. This is possible only if inexpensive transceivers are used. The desired setup is achievable with the hardware developed for the purpose of our system.

C. On-Line Frequency Analysis

In this test, the on-line sampling rate is analyzed during normal operation of the system, i.e. when several devices are changing their locations within the investigated area. The (electromagnetic) devices create interferences, echoes and signal shadows that introduce variability into the measurements.

In this scenario, the transceivers receive many signals but, after analyzing them, only the test device's signal is processed forward by the system. The emission period of the test device is manually changed in each experiment. The number of signal samples (emitted by the test device) measured by six transceivers equaled 200 (M = 200).

Analysis of the on-line sampling rate consists in dividing the 200 samples into 4 groups (K = 4) and comparing the

groups in order to understand whether the samples display stationary or jerky behavior. For this purpose, we calculate F_{exp} as the relation of the variance between groups and the mean variance inside the group. This value is compared with the F-distribution for K-1 (3 in our case) and M-K (196 in our case) degrees of freedom and 0.9-significance level. If $F_{exp} < F_{0.9,3,196}$, then we may conclude that the series has a stationary behavior and the system should reduce the on-line calibration sampling rate.

The tests have been repeated 9 times in order to obtain the confidence intervals of F_{exp}. Changes affecting individual tests depend on the variability of the environment. Nevertheless, taking into account that all tests (for each rate tested) were performed in short time intervals, we may assume similar environment conditions, so the results tend to be Gaussian.

The results and the decision of the algorithm regarding different sampling rates are shown in the first four columns of Table I. The remaining columns of the table show an analysis performed in order to check whether the system should increase the sampling rate. To this end, we compare the jumps between consecutive groups with the mean difference between consecutive single samples, see formula (7). From this comparison, the system concludes whether to increase the sampling rate. By changing the value U, we may tune the minimum value of the sampling rate.

As may be observed from Table I, for the current environmental conditions, the on-line calibration sampling rate adjustment algorithm will maintain a rate of 80 to 160 samples/min.

The table shows that, for some tests, the variance is clearly higher than for others. It is difficult to understand this effect, especially if we take into account that this effect reoccurred in several tests. The unique supposition is that the variability of the environment has a high impact on RSS measurements.

D. Analysis of the Moving Average

Selection of one of the two moving averages: Weighted Moving Average (WMA) or Exponential Moving Average (EMA) has repercussions for the accuracy of positioning. EMA, in particular, attached higher weights to the last calibration measures than WMA. The choice between EMA and WMA depends on the variability of environment conditions, in the same way as does the on-line calibration probing frequency: EMA avoids oscillations under variable environment
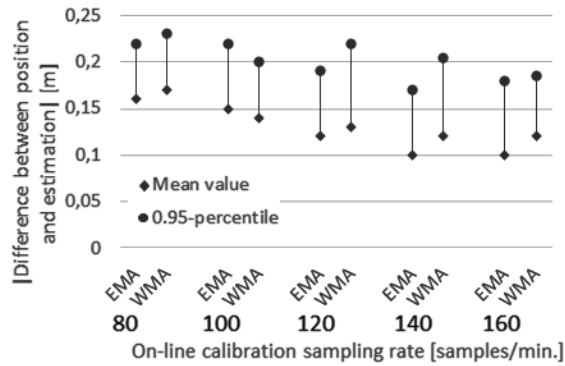
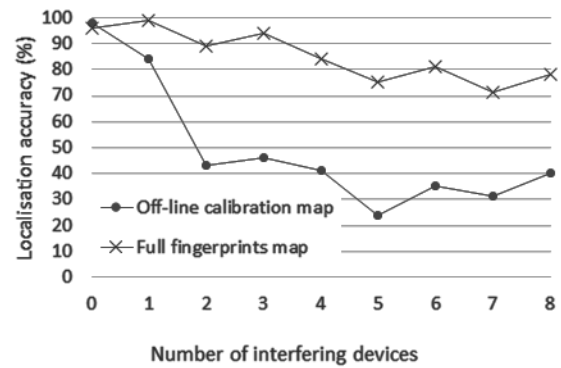Fig. 7. Positioning accuracy vs. on-line calibration sampling rate (EMA-based and WMA-based algorithms).

Fig. 8. Positioning accuracy for an increasing number of interfering devices positioned in the test area (full fingerprints map and off-line only calibration map).

conditions, but it fails in providing information about the reliability of transceivers.

This analysis compares the accuracy of both types of moving averages in previously defined sampling rate intervals. The calibration map does not change during these tests, so it is calculated off-line, shortly before the test is run.

The next figure shows the accuracy of the positioning algorithm for both moving averages and for an increasing measurement sampling rate. Accuracy is calculated as the difference between location and positioning (average and 0.95-percentile). The system works under normal conditions (i.e. with variations in the environment) and the algorithm localizes the test device at least 100 times during each experiment (different positions), using six transceivers.

The effects that moving average has on the accuracy of the positioning system are not substantial, as shown also in Fig. 7, where the differences in accuracy equal 0.05 m, and the difference between 0.05- 0.95-percentiles is only around 0.1 m. However, the results also show that accuracy depends, only slightly, on the sampling rate of on-line calibration measurements.

E. Performance Evaluation and Testing

The last experiments evaluate the system working in its fully operational mode, i.e. a full fingerprints map is being updated in parallel to positioning operations. For on-line calibration measurements, 8 testing devices are situated in the room, send test signals each every 0.5 s (120 samples/min.). Their positions are well known, so the on-line calibration map is updated as explained in the previous section, i.e. based on RSS measurements of the 8 test devices and taking into account the off-line map, the system re-calculates the fingerprints map for all points on the map.

Under these conditions, the accuracy of the system is calculated as follows: a moving test device with a well-known position emits signals which are received and measured by 6 transceivers, so the test device may be localized. The device is tracked in two ways: by using the fingerprints map (which takes into account off-line and on-line calibrations), and by using the off-line calibration map only, so that we may compare the results and understand the effect of on-line calibration. Where the difference between the actual and estimated positions is lower than $0.2\sqrt{2}$ (the fingerprints map is a 0.4m-grid map), then the test result is deemed positive. The accuracy is the relationship between positive results and all test results.

Moreover, other devices (between 1 and 8) were placed in the space under analysis, generating interference and creating radio coverage shadows or echoes. These devices are connected to the Internet (different Internet applications) through a Bluetooth interface. The number of interfering devices is increased from one test to another. It is assumed that the system adapts to the changes in the environment caused by the activity of interfering devices. Such an adaptation is learnt by the calibration process and affects the on-line calibration map. Fig. 8 shows the localization accuracy ratio (see previous paragraph) of a moving test device for an increasing number of interfering devices.

The results show supremacy of the full fingerprints map (which takes into account environmental changes as well) over the off-line calibration map. In some tests, the accuracy increases up to 51%. The accuracy of the system using the full fingerprints map is very high (over 80% in all tests). The accuracy level decreases with the increasing number of interfering devices. However, with calibration being based uniquely on off-line measurements, accuracy deteriorates quickly, whereas on-line calibration achieves significantly higher accuracy values. The bigger the number of interfering devices present in the room, the higher the difference in accuracy between on-line and off-line calibrations.

V. CONCLUSION AND FUTURE WORK

This paper shows the deployment of a localization-based system for industrial applications that includes a multi-technology multi-antenna infrastructure and considers feedback between calibration and positioning processes running in parallel. The system fills the gap between static and dynamic solutions thanks to on-line calibration - a techniques that allows to adapt the calibration map to harsh and changing environment conditions by introducing a feedback mechanism and an estimation algorithm based on the machine learning approach. Although the fingerprint solutions proposed until now show good results in stationary conditions, they fail when

uncertainties arise. Our system has been deployed and tested in close-to-real conditions, where a number of other devices create interferences, shadows and obstacles affecting normal communication. The results show outstanding accuracy levels (in comparison with other existing approaches) and the ability to adapt to ongoing changes in the environment. A distinctive feature of the proposed solution is the use of single transceiver modules (multi-antenna system) for several technologies. This is possible thanks to the fact that the technologies relied upon operate in the same frequency band. In addition, the proposed scheme will only be used in Industrial Internet of Things solutions (no other data requiring high bandwidth will be sent). Another innovative feature is the separation between the functions responsible for radio channel broadcasts and for controlling the transmission. Furthermore, the solution is based on virtualization and introduces modularity - both these features ensure flexibility for future deployments. The result is a system where the area in question is monitored by many transceiver modules, meaning that the costs of the system is reduced.

Based on the implementation of our system, we conducted extensive testbed experiments aiming to analyze the effects of off-line and on-line calibration, and to prove the accuracy of the system.

All experiments aimed to demonstrate the validity of the solution and to compare it with other feasible solutions (e.g. the ones referred to in [47]), which required the best environment conditions (i.e. one testing device). Our future work will be focused on understanding the system's accuracy limits when multiple devices based on different technologies are considered. Therefore, we will provide different fingerprint maps for different technologies, such that the system checks the technology of the device and tries to position it within the fingerprints map specific to that technology. Moreover, our future work aim to develop a communication framework between the positioning system and the on-line testing devices, in order to ensure that the system is capable of automatically adjusting the on-line calibration frequency.

In the near future, we aim to develop our system for large area applications and will try to define the number of on-line devices that have to be deployed for achieving the accuracy level that is required of the system. This will define the final cost of the solution. Moreover, we aim to develop new algorithms for the adaptive positioning system taking advantage of both off- and on-line measurements.

References

[1] S. Jeschke, C. Brecher, H. Song, and D. Rawat, *Industrial Internet of Things: Cybermanufacturing Systems*. Cham, Switzerland: Springer, 2017, pp. 1–715.

[2] X. Cui, T. A. Gulliver, H. Song, and J. Li, "Real-time positioning based on millimeter wave device to device communications," *IEEE Access*, vol. 4, pp. 5520–5530, 2016.

[3] H. Song, D. Rawat, S. Jeschke, and C. Brecher, *Cyber-Physical Systems: Foundations, Principles and Applications*. Boston, MA: Academic, 2016, pp. 1–514.

[4] C. Tang, L. Zhang, Y. Zhang, and H. Song, "Factor graph-assisted distributed cooperative positioning algorithm in the GNSS system," *Sensors*, vol. 18, p. 3748, Nov. 2018.

[5] H. Song, R. Srinivasan, T. Sookoor, and S. Jeschke, *Smart Cities: Foundations, Principles and Applications*. Hoboken, NJ, USA: Wiley, 2017, pp. 1–906.

[6] I. GmbH. (2018). *White Paper: Indoor Positioning Services*. Accessed: Jun. 2019. [Online]. Available: https://www.infsoft.com/portals/0/images/solutions/basics/whitepaper/infsoft-whitepaper-en-indoor-positioning_download.pdf

[7] H. Song and M. Brandt-Pearce, "A 2-D discrete-time model of physical impairments in wavelength-division multiplexing systems," *J. Lightw. Technol.*, vol. 30, no. 5, pp. 713–726, Mar. 1, 2012, doi: 10.1109/JLT.2011.2180360.

[8] L. Zwirello, M. Janson, C. Ascher, U. Schwesinger, G. F. Trommer, and T. Zwick, "Localization in industrial halls via ultra-wideband signals," in *Proc. 7th Workshop Positioning, Navigat. Commun.*, Mar. 2010, pp. 144–149.

[9] S. Holm, "Hybrid ultrasound-RFID indoor positioning: Combining the best of both worlds," in *Proc. IEEE Int. Conf. RFID*, Apr. 2009, pp. 155–162.

[10] M. Hölzl, R. Neumeier, and G. Ostermayer, "Localization in an industrial environment: A case study on the difficulties for positioning in a harsh environment," *Int. J. Distrib. Sensor Netw.*, vol. 11, no. 8, Aug. 2015, Art. no. 567976, doi: 10.1155/2015/567976.

[11] A. Lewandowski and C. Wietfeld, "A comprehensive approach for optimizing ToA-localization in harsh industrial environments," in *Proc. IEEE/ION Position, Location Navigat. Symp.*, May 2010, pp. 516–525.

[12] Y. Sun, H. Song, A. J. Jara, and R. Bie, "Internet of Things and big data analytics for smart and connected communities," *IEEE Access*, vol. 4, pp. 766–773, 2016, doi: 10.1109/ACCESS.2016.2529723.

[13] H. Choi, H. Jin, and S. C. Kim, "RSS bias compensation in BLE beacon based positioning system," in *Proc. 9th Int. Conf. Ubiquitous Future Netw. (ICUFN)*, Milan, Italy, Jul. 2017, pp. 494–497.

[14] S. Sahin, H. Ozcan, and K. Kucuk, "Smarttag: An indoor positioning system based on smart transmit power scheme using active tags," *IEEE Access*, vol. 6, pp. 23500–23510, Apr. 2018.

[15] L. Khalil, A. Waadt, G. Bruck, and P. Jung, "Positioning framework for WLAN 802.11n utilizing Kalman filter on received signal strength," in *Proc. Int. Wireless Commun. Mobile Comput. Conf. (IWCMC)*, Nicosia, Cyprus, Aug. 2014, pp. 1172–1176.

[16] H. Laitinen, S. Juurakko, T. Lahti, R. Korhonen, and J. Lahteenmaki, "Experimental evaluation of location methods based on signal-strength measurements," *IEEE Trans. Veh. Technol.*, vol. 56, no. 1, pp. 287–296, Jan. 2007.

[17] P. Pivato, L. Palopoli, and D. Petri, "Accuracy of RSS-based centroid localization algorithms in an indoor environment," *IEEE Trans. Instrum. Meas.*, vol. 60, no. 10, pp. 3451–3460, Oct. 2011.

[18] J. Yim, "Introducing a decision tree-based indoor positioning technique," *Expert Syst. Appl.*, vol. 34, no. 2, pp. 1296–1302, 2008.

[19] F. Potorti, A. Crivello, M. Girolami, E. Traficante, and P. Barsocchi, "Wi-Fi probes as digital crumbs for crowd localisation," in *Proc. Int. Conf. Indoor Positioning Indoor Navigat. (IPIN)*, Alcala de Henares, Spain, Oct. 2016, pp. 1–8.

[20] S. U. Rehman, K. W. Sowerby, S. Alam, and I. Ardekani, "Radio frequency fingerprinting and its challenges," in *Proc. IEEE Conf. Commun. Netw. Secur.*, San Francisco, CA, USA, Oct. 2014, pp. 496–497.

[21] D. V. Le, N. Meratnia, and P. J. M. Havinga, "Unsupervised deep feature learning to reduce the collection of fingerprints for indoor localization using deep belief networks," in *Proc. Int. Conf. Indoor Positioning Indoor Navigat. (IPIN)*, Nantes, France, Sep. 2018, pp. 1–7.

[22] S. Tomažic, D. Dovžan, and I. Škrjanc, "Confidence-interval fuzzy model-based indoor localization," *IEEE Trans. Ind. Electron.*, vol. 66, no. 3, pp. 2015–2024, Jun. 2018.

[23] K. Youssef, L. Bouchard, K. Haigh, J. Silovsky, B. Thapa, and C. V. Valk, "Machine learning approach to RF transmitter identification," *IEEE J. Radio Freq. Identificat.*, vol. 2, no. 4, pp. 197–205, Dec. 2018.

[24] J. Kim and D. Han, "Passive WiFi fingerprinting method," in *Proc. Int. Conf. Indoor Positioning Indoor Navigat. (IPIN)*, Nantes, France, Sep. 2018, pp. 1–8.

[25] Nextome Co. (Jul. 2017). *Indoor Positioning and Navigation System*. [Online]. Available: https://www.nextome.net/

[26] C. Pendão and A. Moreira, "FastGraph–Organic 3D graph for unsupervised location and mapping," in *Proc. Int. Conf. Indoor Positioning Indoor Navigat. (IPIN)*, Sep. 2018, pp. 206–212.

[27] P. Bahl and V. N. Padmanabhan, "RADAR: An in-building RF-based user location and tracking system," in *Proc. IEEE INFOCOM Conf. Comput. Commun., 19th Annu. Joint Conf. IEEE Comput. Commun. Societies*, vol. 2, Mar. 2000, pp. 775–784.

[28] A. del Corte-Valiente, J. Manuel GóMEZ-PULIDO, and O. Gutiérrez-Blanco, "Efficient techniques and algorithms for improving indoor localization precision on WLAN networks applications," *Int. J. Commun., Netw. Syst. Sci.*, vol. 02, no. 07, pp. 645–651, 2009.

[29] A. Ettlinger and G. Retscher, "Positioning using ambient magnetic fields in combination with Wi-Fi and RFID," in *Proc. Int. Conf. Indoor Positioning Indoor Navigat. (IPIN)*, Alcala de Henares, Spain, Oct. 2016, pp. 1–8.

[30] G. M. Reis, H. León, T. Alam, J. Anderson, L. Bobadilla, and R. N. Smith, "A whitening-based tracking algorithm for autonomous underwater vehicles," in *Proc. OCEANS - MTS/IEEE Kobe Techno-Oceans (OTO)*, Kobe, Japan, May 2018, pp. 1–6.

[31] Y.-K. Kim, S.-H. Choi, and J.-M. Lee, "Enhanced outdoor localization of multi-GPS/INS fusion system using Mahalanobis distance," in *Proc. 10th Int. Conf. Ubiquitous Robots Ambient Intell. (URAI)*, Jeju, South Korea, Oct. 2013, pp. 488–492.

[32] Q. Yang and Z. Bian, "A metric learning model for localization," in *Proc. IEEE Adv. Inf. Manage., Communicates, Electron. Automat. Control Conf. (IMCEC)*, Xi'an, China, Oct. 2016, pp. 1137–1141.

[33] X. Chen and Z. J. Wang, "Reliable indoor location sensing technique using active RFID," in *Proc. 2nd Int. Conf. Ind. Mechatronics Automat.*, Vancouver, BC, Canada, 2010, pp. 160–163.

[34] Y. Gu, A. Lo, and I. Niemegeers, "A survey of indoor positioning systems for wireless personal networks," *IEEE Commun. Surveys Tuts.*, vol. 11, no. 1, pp. 13–32, 1st Quart., 2009.

[35] D. Ksentini, A. R. Elhadi, and N. Lasla, "Inertial measurement unit: Evaluation for indoor positioning," in *Proc. Int. Conf. Adv. Netw. Distrib. Syst. Appl.*, Jun. 2014, pp. 25–30.

[36] Z. Jiangy, W. Xiy, X.-Y. Li, J. Zhaoy, and J. Hany, "HiLoc: A TDoA fingerprint hybrid indoor localization system," Microsoft Indoor Localization Competition, Tech. Rep., 2014. Accessed: Mar. 2020. [Online]. Available: https://www.microsoft.com/en-us/research/wp-content/uploads/2013/09/ipsn.pdf

[37] A. K. M. M. Hossain and W.-S. Soh, "A comprehensive study of bluetooth signal parameters for localization," in *Proc. IEEE 18th Int. Symp. Pers., Indoor Mobile Radio Commun.*, Sep. 2007, pp. 1–5.

[38] M. Ji, J. Kim, J. Jeon, and Y. Cho, "Analysis of positioning accuracy corresponding to the number of BLE beacons in indoor positioning system," in *Proc. 17th Int. Conf. Adv. Commun. Technol. (ICACT)*, 2015, pp. 92–95.

[39] D. Čabarkapa, I. Grujić, and P. Pavlović, "Comparative analysis of the Bluetooth low-energy indoor positioning systems," in *Proc. 12th Int. Conf. Telecommun. Mod. Satell., Cable Broadcast. Services (TELSIKS)*, 2015, pp. 76–79.

[40] R. Dobbins, S. E. Garcia, and B. Shaw, "Software defined radio localization using 802.11-style communications," Dept. Worcester Polytech. Inst., A Major Qualifying Project Rep., 2011. Accessed: Mar. 2020. [Online]. Available: https://digitalcommons.wpi.edu/cgi/viewcontent.cgi?article=4135&context=mqp-all

[41] T. Vaupel, J. Seitz, F. Kiefer, S. Haimerl, and J. Thielecke, "Wi-Fi positioning: System considerations and device calibration," in *Proc. Int. Conf. Indoor Positioning Indoor Navigat.*, Sep. 2010, pp. 1–7.

[42] H. Othman, N. At, and C. Topal, "Effectiveness of online RF finger-printing for indoor localization," in *Proc. 26th Signal Process. Commun. Appl. Conf. (SIU)*, Izmir, Turkey, May 2018, pp. 1–4.

[43] A. Ye, X. Yang, L. Xu, and Q. Li, "A novel adaptive radio-map for RSS-based indoor positioning," in *Proc. Int. Conf. Green Inform. (ICGI)*, Fuzhou, China, Aug. 2017, pp. 205–210, doi: 10.1109/ICGI.2017.9.

[44] S. H. Fang, Y. C. Cheng, and Y. R. Chien, "Exploiting sensed radio strength and precipitation for improved distance estimation," *IEEE Sensors J.*, vol. 18, no. 16, pp. 6863–6873, Aug. 2018.

[45] D. Slock, "Diversity aspects of power delay profile based location fingerprinting," in *Proc. IEEE Int. Conf. Acoust., Speech Signal Process. (ICASSP)*, Kyoto, Japan, Mar. 2012, pp. 2861–2864.

[46] R. Faragher and R. Harle, "An analysis of the accuracy of bluetooth low energy for indoor positioning applications," in *Proc. 27th Int. Tech. Meeting Satell. Division Inst. Navigat. (ION GNSS+)*, Tallahassee, FL, USA, 2014, pp. 1–10.

[47] D. Lymberopoulos, J. Liu, X. Yang, R. R. Choudhury, S. Sen, and V. Handziski, "Microsoft indoor localization competition: Experiences and lessons learned," *GetMobile, Mobile Comput. Commun.*, vol. 18, no. 4, pp. 24–31, Oct. 2014.

[48] J. Torres-Sospedra *et al.*, "Off-line evaluation of mobile-centric indoor positioning systems: The experiences from the 2017 IPIN competition," *Sensors*, vol. 18, no. 2, p. 487, 2018.

[49] W. Burakowski, "Provision of end-to-end QoS in heterogeneous multi-domain networks," *Ann. Telecommun.*, vol. 63, no. 11, pp. 559–577, 2008.

[50] J. M. Batalla, G. Mastorakis, C. X. Mavromoustakis, and J. Zurek, "On cohabitating networking technologies with common wireless access for home automation system purposes," *IEEE Wireless Commun.*, vol. 23, no. 5, pp. 76–83, Oct. 2016.

[51] C. X. Mavromoustakis, J. M. Batalla, G. Mastorakis, E. Markakis, and E. Pallis, "Socially oriented edge computing for energy awareness in IoT architectures," *IEEE Commun. Mag.*, vol. 56, no. 7, pp. 139–145, Jul. 2018.

[52] J. M. Batalla and F. Gonciarz, "Deployment of smart home management system at the edge: Mechanisms and protocols," *Neural Comput. Appl.*, vol. 31, no. 5, pp. 1301–1315, Jun. 2018.

[53] J. M. Batalla, A. Vasilakos, and M. Gajewski, "Secure smart homes: Opportunities and challenges," *ACM Comput. Surv.*, vol. 50, no. 5, pp. 1–32, Oct. 2017.

[54] J. M. Batalla, M. Gajewski, W. Latoszek, P. Krawiec, C. Mavromoustakis, and G. Mastorakis, "ID-based service-oriented communications for unified access to IoT," *Comput. Elect. Eng.*, vol. 52, pp. 98–113, May 2016.

[55] N. J. LaSorte, S. A. Rajab, and H. H. Refai, "Experimental assessment of wireless coexistence for 802.15.4 in the presence of 802.11g/n," in *Proc. IEEE Int. Symp. Electromagn. Compat.*, Aug. 2012, pp. 473–479.

[56] F. Zafari, A. Gkelias, and K. K. Leung, "A survey of indoor localization systems and technologies," *IEEE Commun. Surveys Tuts.*, vol. 21, no. 3, pp. 2568–2599, 3rd Quart., 2019.

[57] W. Sakpere, M. Adeyeye Oshin, and N. B. Mlitwa, "A state-of-the-art survey of indoor positioning and navigation systems and technologies," *South Afr. Comput. J.*, vol. 29, no. 3, 2017.

[58] L. Zhu, A. Yang, D. Wu, and L. Liu, "Survey of indoor positioning technologies and systems," in *Proc. Life Syst. Modelling Simulation*, 2014, pp. 400–409.

Jordi Mongay Batalla is with the Warsaw University of Technology, where he is also an Associate Professor. He is currently the Research Director of the National Institute of Telecommunications, Poland. His research interests focuses mainly on technologies (radio: 4G and 5G, wired: Network services chain, SDN) and applications (Internet of Things, Smart Cities, multimedia) for the Future Internet. He has written more than 100 research papers in renowned international journals and conferences, and is on the Editorial Boards of several journals.

Constandinos X. Mavromoustakis is currently a Professor with the Department of Computer Science, University of Nicosia, Cyprus, where he is leading the Mobile Systems Laboratory, Department of Computer Science, University of Nicosia. He has been an Active Member (currently serves as the Chair) of the IEEE/R8 regional Cyprus Section since January 2016. Since May 2009, he serves as the Chair for the C16 Computer Society Chapter of the Cyprus IEEE Section.

George Mastorakis received the B.Eng. (Hons.) degree from the University of Manchester Institute of Science and Technology (UMIST), the M.Sc. degree from University College London (UCL), and the Ph.D. degree from the University of the Aegean. He is currently an Associate Professor with Hellenic Mediterranean University and the Director of the E-Business Intelligence Laboratory. His research interests include cognitive radio networks, energy-efficient networks, IoT, Big Data, network traffic analysis, and radio resource management.

Neal Naixue Xiong received the Ph.D. degree from the Japan Advanced Institute of Science and Technology. Before he attends SWOSU, he worked in Colorado Technical University (Full Professor, four years), Wentworth Institution of Technology, and Georgia State University for many years. He is currently with the Department of Business and Computer Science, Southwestern Oklahoma State University (SWOSU), OK, USA. His research interests include cloud computing, business networks, security and dependability, parallel and distributed computing, and optimization theory. He has published over 100 international journal articles and over 100 international conference articles.

Jozef Wozniak (Senior Member, IEEE) received the Ph.D. and D.Sc. degrees in electronics and telecommunications from the Gdansk University of Technology (GUT). He is currently a Full Professor with the Faculty of Electronics, Telecommunications and Computer Science, GUT. He has participated in various research and teaching activities, including visits at Vrije Universiteit Brussel, Politecnico di Milano, and Aalborg University, Denmark. In 2006, he was invited to Canterbury University, Christchurch, New Zealand, as a Visiting Erskine Fellow. He has been a TPC member for a number of national and international conferences, also chairing or co-chairing several of them. He was the Organizer and Chair of the Computer Society Chapter at GUT. From 2013 to 2018, he was chairing the Working Group 6.8 (Wireless and Mobile Communications) of IFIP TC6.